ETSI GR RIS 006 V1.1.1 (2025-06)

GROUP REPORT

Reconfigurable Intelligent Surfaces (RIS); Multi-functional Reconfigurable Intelligent Surfaces (RIS): Modelling, Optimization, and Operation

Reference
DGR/RIS-006

Keywords
model, radio, RIS

ETSI

650 Route des Lucioles
F-06921 Sophia Antipolis Cedex - FRANCE

Tel.: +33 4 92 94 42 00   Fax: +33 4 93 65 47 16

Siret N° 348 623 562 00017 - APE 7112B
Association à but non lucratif enregistrée à la
Sous-Préfecture de Grasse (06) N° w061004871

Contents

Intellectual Property Rights

Essential patents

IPRs essential or potentially essential to normative deliverables may have been declared to ETSI. The declarations pertaining to these essential IPRs, if any, are publicly available for **ETSI members and non-members**, and can be found in ETSI SR 000 314: *"Intellectual Property Rights (IPRs); Essential, or potentially Essential, IPRs notified to ETSI in respect of ETSI standards"*, which is available from the ETSI Secretariat. Latest updates are available on the ETSI IPR online database.

Pursuant to the ETSI Directives including the ETSI IPR Policy, no investigation regarding the essentiality of IPRs, including IPR searches, has been carried out by ETSI. No guarantee can be given as to the existence of other IPRs not referenced in ETSI SR 000 314 (or the updates on the ETSI Web server) which are, or may be, or may become, essential to the present document.

Trademarks

The present document may include trademarks and/or tradenames which are asserted and/or registered by their owners. ETSI claims no ownership of these except for any which are indicated as being the property of ETSI, and conveys no right to use or reproduce any trademark and/or tradename. Mention of those trademarks in the present document does not constitute an endorsement by ETSI of products, services or organizations associated with those trademarks.

DECT™, **PLUGTESTS™**, **UMTS™** and the ETSI logo are trademarks of ETSI registered for the benefit of its Members. **3GPP™**, **LTE™** and **5G™** logo are trademarks of ETSI registered for the benefit of its Members and of the 3GPP Organizational Partners. **oneM2M™** logo is a trademark of ETSI registered for the benefit of its Members and of the oneM2M Partners. **GSM**® and the GSM logo are trademarks registered and owned by the GSM Association.

Foreword

This Group Report (GR) has been produced by ETSI Industry Specification Group (ISG) Reconfigurable Intelligent Surfaces (RIS).

Modal verbs terminology

In the present document "**should**", "**should not**", "**may**", "**need not**", "**will**", "**will not**", "**can**" and "**cannot**" are to be interpreted as described in clause 3.2 of the ETSI Drafting Rules (Verbal forms for the expression of provisions).

"**must**" and "**must not**" are **NOT** allowed in ETSI deliverables except when used in direct citation.

1 Scope

The present document is to:

a) identify technological challenges and summarize technical solutions for MF-RIS incorporating transmission, reflection, sensing, computation, and other potential functions;

b) study channel modelling, coefficient optimization, deployment design, resource allocation and other technical aspects of MF-RIS;

c) suggest possible ways of deploying MF-RIS in real-world scenarios and the expected performance enhancement in different scenarios.

2 References

2.1 Normative references

Normative references are not applicable in the present document.

2.2 Informative references

References are either specific (identified by date of publication and/or edition number or version number) or non-specific. For specific references, only the cited version applies. For non-specific references, the latest version of the referenced document (including any amendments) applies.

NOTE: While any hyperlinks included in this clause were valid at the time of publication, ETSI cannot guarantee their long-term validity.

The following referenced documents may be useful in implementing an ETSI deliverable or add to the reader's understanding, but are not required for conformance to the present document.

[i.1] ETSI GR RIS 001: "Reconfigurable Intelligent Surfaces (RIS); Use Cases, Deployment Scenarios and Requirements".

[i.2] ETSI GR RIS 003: "Reconfigurable Intelligent Surfaces (RIS); Communication Models, Channel Models, Channel Estimation and Evaluation Methodology".

[i.3] X. Mu, et al.: "Simultaneously Transmitting and Reflecting (STAR) RIS Aided Wireless Communications", in IEEE™ Transactions on Wireless Communications, vol. 21, no. 5, pp. 3083-3098, May 2022.

[i.4] Y. Liu, et al.: "Simultaneously Transmitting and Reflecting (STAR)-RISs: A Coupled Phase-Shift Model", ICC 2022 - IEEE™ International Conference on Communications, Seoul, Korea, Republic of, 2022, pp. 2840-2845.

[i.5] R. Liu, J. Dou, P. Li, J. Wu and Y. Cui: "Simulation and Field Trial Results of Reconfigurable Intelligent Surfaces in 5G Networks", in IEEE™ Access, vol. 10, pp. 122786-122795, 2022.

[i.6] R. Zhong, et al.: "STAR-RISs Assisted NOMA Networks: A Distributed Learning Approach", in IEEE™ Journal of Selected Topics in Signal Processing, vol. 17, no. 1, pp. 264-278, January 2023.

[i.7] Q. Wu, et al.: "Intelligent surfaces empowered wireless network: Recent advances and the road to 6G", in Proceedings of the IEEE™, vol. 112, no. 7, pp. 724-763, July 2024.

[i.8] X. Shao, et al.: "Target Sensing With Intelligent Reflecting Surface: Architecture and Performance", in IEEE™ Journal on Selected Areas in Communications, vol. 40, no. 7, pp. 2070-2084, July 2022.

[i.9] ETSI GR RIS 002: "Reconfigurable Intelligent Surfaces (RIS); Technological challenges, architecture and impact on standardization".

[i.10] Z. Wang, et al.: "STARS Enabled Integrated Sensing and Communications", in IEEE™ Transactions on Wireless Communications, vol. 22, no. 10, pp. 6750-6765, October 2023.

[i.11] Q. Peng, et al.: "Semi-passive intelligent reflecting surface enabled sensing systems", in IEEE™ Transactions on Communications, vol. 72, no. 12, pp. 7674-7688, Dec. 2024.

[i.12] M. Hua, et al.: "Intelligent reflecting surface assisted localization: Performance analysis and algorithm design", in IEEE™ Wireless Communications Letters, vol. 13, no. 1, pp. 84-88, January 2024.

[i.13] K. Meng, et al.:"Sensing-Assisted Communication in Vehicular Networks with Intelligent Surface", in IEEE™ Transactions on Vehicular Technology, vol. 73, no. 1, pp. 876-893, January 2024.

[i.14] E. Björnson, et al.: "Reconfigurable Intelligent Surfaces: A signal processing perspective with wireless applications", in IEEE™ Signal Processing Magazine, vol. 39, no. 2, pp. 135-158, March 2022.

[i.15] C. Ouyang, et al.: "Integrated Sensing and Communications: A Mutual Information-Based Framework", in IEEE™ Communications Magazine, vol. 61, no. 5, pp. 26-32, May 2023.

[i.16] J. An, et al.: "Stacked Intelligent Metasurface-Aided MIMO Transceiver Design", in IEEE™ Wireless Communications, vol. 31, no. 4, pp. 123-131, August 2024.

[i.17] Z. Hu, et al.: "Caching-at-STARS: the Next Generation Edge Caching", in IEEE™ Transactions on Wireless Communications, vol. 23, no. 8, pp. 8372-8387, August 2024.

3 Definition of terms, symbols and abbreviations

3.1 Terms

Void.

3.2 Symbols

Void.

3.3 Abbreviations

For the purposes of the present document, the following abbreviations apply:

AoA Angles of Arrival
AP Acces Point
BS Base Station
CRLB Cramér-Rao Lower Bound
CSI Channel State Information
DFT Discrete Fourier Transform
DoA Direction of Angle
DoF Degrees of Freedom
EM ElectroMagnetic
ES Energy Splitting
IMT International Mobile Telecommunication
ISAC Integrated Sensing And Communication
JO Joint Optimization
LoS Line of Sight
MF-RIS Multi-Functional Reconfigurable Intelligent Surfaces
MIMO Multiple-Input Multiple-Output
NCJT Non-Coherent Joint Transmission
NOMA Non-Orthogonal Multiple Access

O2I	Outdoor-to-Indoor
RF	Radio Frequencies
RIS	Reconfigurable Intelligent Surfaces
RoI	Region of Interest
S&C	Sensing and Communication
SIM	Stacked Intelligent Metasurfaces
SINR	Signal-to-Interference-plus-Noise Ratio
SNR	Signal-to-Noise Ratio
SS	Surface Splitting
SSB	Synchronization Signal Block
STAR	Simultaneously Transmitting And Reflecting
TDM	Time Division Mode
ToA	Time of Arrival
TS	Time Switching
UE	Use Equipment

4 General aspects of MF-RIS

4.0 General Introduction of MF-RIS

Following the general definition of RIS in clause 4 of ETSI GR RIS 001 [i.1], RIS integrated with multiple functionalities (e.g. transmission (refraction)), reflection, sensing, computing, and caching), namely MF-RIS, is discussed in the present document with their signal modelling, operating protocols, possible deployment considerations, RIS coefficients design, and performance analysis. Here, the different types of MF-RIS to be discussed are listed as below:

- **STAR RIS:** This is an RIS that integrate the two fundamental transmission (refraction) and reflection functions into one single surface, which can forward the incident wireless signals into both sides of the RIS, i.e. achieving a full-space coverage.
- **RIS with sensing capabilities:** This is an RIS that integrates active sensors to detect the surrounding targets and/or feedback the sensing results to the base stations or users.
- **RIS with computing capabilities:** This is an RIS that achieves dedicated signal processing tasks (e.g. precoding and signal detection) during the wireless signal passing through the surface.
- **RIS with caching capabilities:** This is an RIS that is installed with caching memory to provide content delivery service to end users.

5 Simultaneously transmitting and reflecting RIS

5.0 General Introduction

STAR RIS is a tunable surface that integrates the transmission (refraction) and reflection functions. As depicted in Figure 5.0-1, the wireless signal incident upon the STAR RIS can be simultaneously transmitted and reflected into the two sides with modified angles. There are various tunable surface designs that are potential candidates for realizing STAR RIS. In terms of periodic structure, STAR RIS hardware implementations can be loosely divided into two categories, namely, patch-array-based implementations and metasurface-based implementations. Patch-array-based implementations consist of periodic cells with sizes on the order of a few centimetres. Because of their relatively large sizes, each cell (patch) can be made tunable by incorporating positive-intrinsic-negative diodes or delay lines. By contrast, metasurface-based implementations have periodic cells on the order of a few millimetres, possibly micrometres, and even molecular sizes. Hence, they require more sophisticated controls of their EM properties, such as conductivity and permittivity. The candidate materials include but not limited to smart glass, graphene, etc.

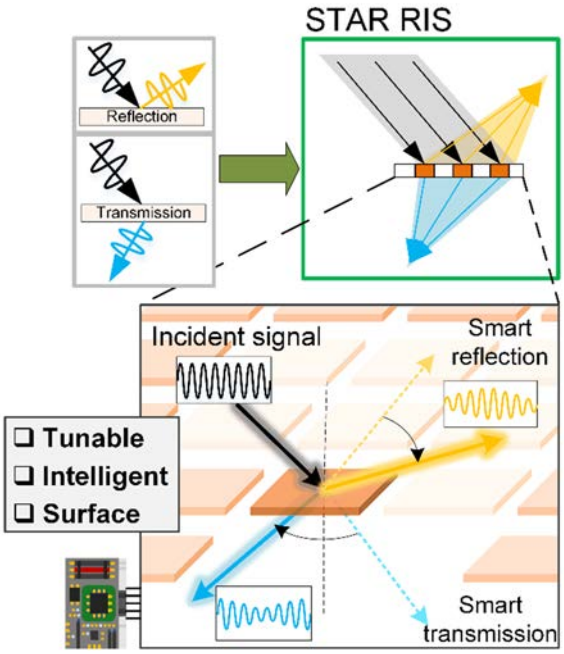

Figure 5.0-1: Illustration of the STAR RIS concept

5.1 Signal and Channel Model

5.1.1 Signal Models for STAR RIS

By exploiting the field equivalence principle, each STAR RIS element is excited by the incident signal, the transmitted and reflected signals can be equivalently treated as waves radiated from the time-varying surface equivalent electric currents $\boldsymbol{J}_p$ and equivalent magnetic currents $\boldsymbol{J}_b$, as shown in Figure 5.1-1. For the *m*-th element, the strengths and distribution of these surface equivalent currents are determined by the incident narrowband signal s_m as well as the local surface averaged electric and magnetic impedances Y_m and Z_m. Let s_m denote the signal incident upon the *m*-th element. Assume that the STAR RIS produces both transmitted and reflected signals, namely t_m and r_m, with the same polarization, these signals can be expressed as:

$$t_m = T_m s_m, \quad r_m = R_m s_m,$$

where T_m and R_m are the transmission and reflection coefficients of the *m*-th element, respectively. According to the law of energy conservation, for passive STAR RIS elements, the following constraint on the local transmission and reflection coefficients are satisfied:

$$|T_m|^2 + |R_m|^2 \leq 1.$$

According to electromagnetic theory, the phase delays of both the transmitted and reflected field are related to Y_m and Z_m. In Figure 5.1-1, the reconfigurability of the element is reflected in the change of the surface impedances, since the transmission and reflection coefficients of the *m*-th element is related to the surface impedances as follows:

$$T_m = \frac{2-\eta_0 Y_m}{2+\eta_0 Y_m} - R_m,$$

$$R_m = -\frac{2\left(\eta_0^2 Y_m - Z_m\right)}{(2+\eta_0 Y_m)(2\eta_0 + Z_m)},$$

where η_0 is the impedance of free space. To facilitate the design of STAR RIS in wireless communication systems, the transmission and reflection coefficients of the *m*-th element can be further rewritten in the form of their amplitudes and phase shifts as follows:

$$T_m = \sqrt{\beta_m^T} e^{j\theta_m^T}, \quad R_m = \sqrt{\beta_m^R} e^{j\theta_m^R},$$

where $\beta_m^T \in [0,1]$ and $\beta_m^R \in [0,1]$ are real-valued amplitude coefficients for transmission and reflection. $\theta_m^T \in [0, 2\pi)$ and $\theta_m^R \in [0, 2\pi)$ are the phase shifts introduced by the m-th element for the transmitted and reflected signals. Here, due to the law of energy conservation, $\beta_m^T + \beta_m^R \leq 1$.

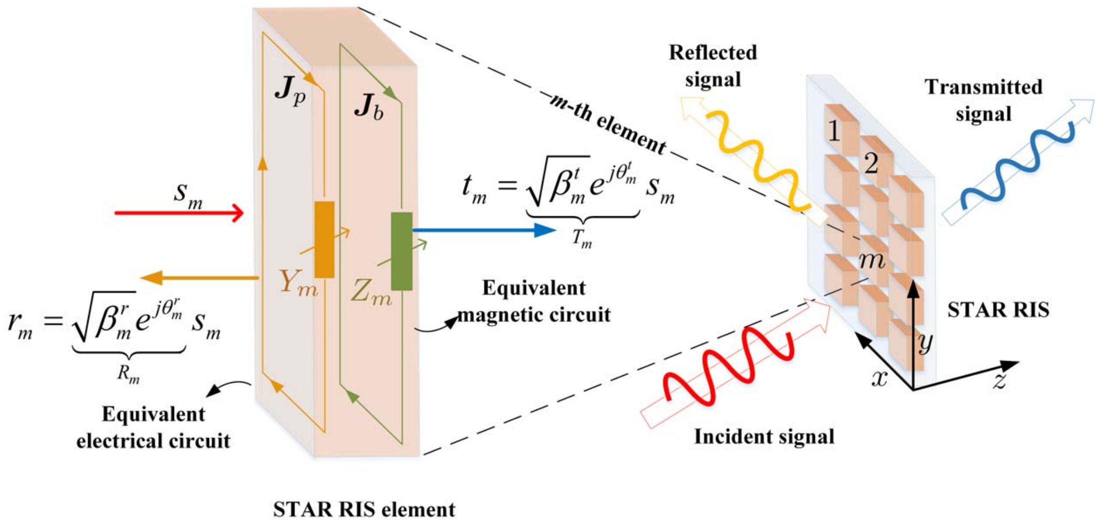

Figure 5.1-1: Schematic illustration of STAR RIS

The value of transmission and reflection coefficients (T_m and R_m) are determined by the two complex-valued impedances, Y_m and Z_m, i.e. tuning surface electric and magnetic impedances. In terms of the phase-shift adjustment capabilities, there are two main categories of phase-shift models for STAR RIS:

- **Independent phase-shift model:** For this STAR RIS, the transmission phase shift (θ_m^T) and the reflection phase shift (θ_m^R) can be adjusted independently with each other. The independent phase-shift model has the maximum DoF for communication design. However, the independent phase-shift model is challenging to realize in practice, especially for passive STAR RIS. This is because if STAR RIS is made of passive materials, the corresponding electric impedance (Y_m) and magnetic impedance (Z_m) cannot be arbitrary values.

- **Coupled phase-shift model:** For STAR RIS using passive lossless materials, the corresponding electric impedance and magnetic impedances should be purely imaginary numbers. Under this constraint, the transmission phase shift (θ_m^T) and the reflection phase shift (θ_m^R) are coupled subject to specific values of phase-shift differences as follows:

$$|\theta_m^T - \theta_m^R| = \frac{1}{2}\pi \; or \; \frac{3}{2}\pi.$$

5.1.2 Channel Models for STAR RIS

For channels associated with STAR RIS, they follow the channel models presented in clause 7 of ETSI GR RIS 003 [i.2].

5.2 Operating Protocols

By adjusting the amplitude coefficients used for both transmission and reflection, each STAR RIS element can operate in full transmission mode (referred to as the T mode), full reflection mode (referred to as the R mode), or simultaneous transmission and reflection mode (referred to as the T&R mode). As shown in Figure 5.2-1, by exploiting such adjustment capabilities, at least three operating protocols can be used to deploy the STAR RIS:

- **Energy Splitting (ES):** For ES, all elements of the STAR RIS are assumed to operate in T&R mode, as shown in Figure 5.2-1(1). For given transmission and reflection amplitude coefficients, the signals incident upon each element are split into transmitted and reflected signals having different energy. In a practical implementation, the amplitude (β_m^T, β_m^R) and phase-shift coefficients (θ_m^T, θ_m^R) of each element for transmission and reflection can be optimized jointly for achieving diverse design objectives in wireless networks.

- **Surface Splitting (SS):** In SS, all elements of the STAR RIS are partitioned into two or more groups. Specifically, one group contains the elements that operate in T mode, while the other group contains the elements operating in R mode. It is possible to have another group, comprising of elements without any phase shift. The surface can be split into many groups, potentially serving different user devices. As shown in Figure 5.2-1(2), a SS STAR RIS can be viewed as being composed of a conventional reflecting-only RIS and a transmitting-only RIS of reduced sizes. Under this protocol, the element-wise mode selection and the corresponding transmission and reflection phase shift coefficients can be optimized jointly. The drawback is that under this mode, the transmission and reflection gain is reduced since only a subset of the elements are selected for transmission and reflection.

- **Time Switching (TS):** The STAR RIS employing the TS protocol periodically switches all elements between T mode and R mode in orthogonal time slots (referred to as T period and R period), as illustrated in Figure 5.2-1(3). The fraction of time allocated to fully transmitting and fully reflecting signals can be optimized to achieve a balance between the communication qualities of the front and back sides. Compared to ES and SS, the advantage of TS is that, for a given time allocation, the transmission and reflection coefficients are not coupled; hence, they can be optimized independently. Nevertheless, periodically switching the elements imposes stringent time synchronization requirements, thus increasing the implementation complexity compared to the ES and SS, as well as potential power consumption.

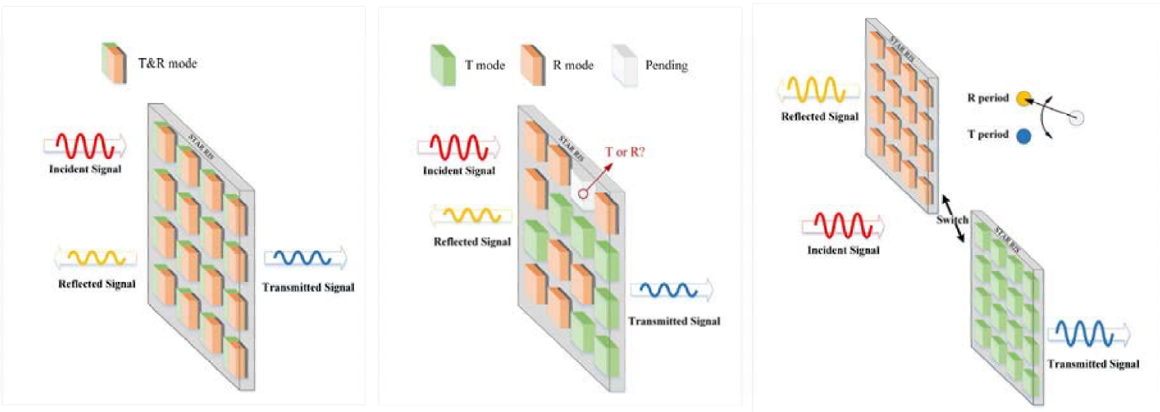

(1) Energy Splitting (2) Surface Splitting (3) Time Switching

Figure 5.2-1: Illustration of three possible protocols for operating STAR RIS

5.3 Reconfigurable Coefficient Design

5.3.0 General

Reconfigurable coefficient design, also known as passive beamforming design, is important to unlock the full benefits of STAR RIS in wireless communications. Note that depending on the near-field or far-field channel models considered, the beamforming can exhibit either beamfocusing or beamsteering characteristic. For a pre-configured communication system, where the BS is connected with the STAR RIS via a controller, a general STAR beamforming design problem can be expressed as follows:

$$\underset{\{\beta_m^T,\beta_m^R,\theta_m^T,\theta_m^R\}}{\frac{\text{maximize}}{\text{minimze}}} \quad \rho(\beta_m^T, \beta_m^R, \theta_m^T, \theta_m^R, X)$$

$$s.t. \;\; \beta_m^T + \beta_m^R \le 1, \theta_m^T \in [0, 2\pi), \theta_m^R \in [0, 2\pi),$$

$$|\theta_m^T - \theta_m^R| = \frac{1}{2}\pi \; or \; \frac{3}{2}\pi, if\ the\ coupled\ phase - shift\ model\ is\ considered,$$

$$Other\ constraints.$$

Here, X represents the set of other optimization variables that are not relevant to STAR RIS, such as user power allocation and BS active beamforming vectors. Despite different operating protocols impose different constraints on the STAR beamforming design problem, the beamforming design in ES STAR RIS is much more challenging than that in SS STAR RIS and TS STAR RIS. The case becomes even worse when considering the coupled phase-shift model. Therefore, tailored passive beamforming algorithms are required. Note that the accurate CSI is essential for the passive beamforming design. For STAR RIS, the CSI can be subsequently obtained by exploiting the TS protocol and CSI estimation methods in clause 8 of ETSI GR RIS 003 [i.2]. In the following, the passive beamforming design is discussed assuming perfect CSI.

5.3.1 Joint Optimization Based STAR Beamforming for the Independent Phase-Shift Model

For ES STAR RIS-assisted communication systems with the independent phase-shift model. the main challenge lies in the coupling between the newly introduced STAR beamforming and the existing variables (e.g. BS active beamforming and power allocation). One existing way is to decompose the original joint BS and RIS beamforming problem into two subproblems and alternatingly optimizes one beamforming with the other fixed. Alternatively, an efficient JO-based beamforming approach is developed for minimizing the BS power consumption in a STAR RIS-assisted multiple-input single-output multi-user communication system [i.3]. As shown in Figure 5.3-1, the BS beamforming and STAR beamforming in the JO-based approach can be simultaneously optimized in each iteration.

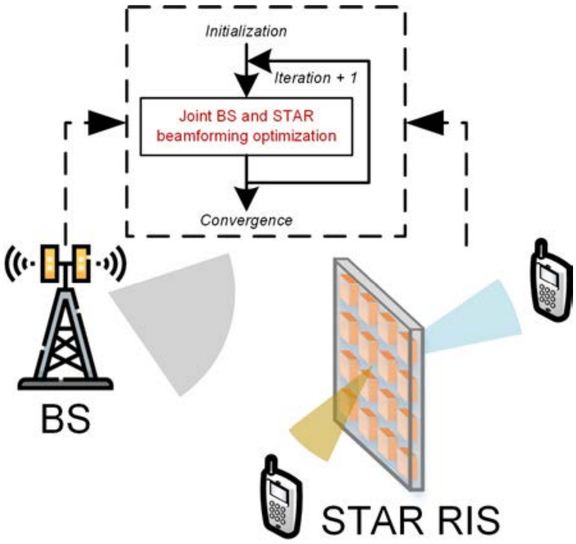

Figure 5.3-1: Joint optimization based STAR beamforming design

5.3.2 Element-Wise Based STAR Beamforming for the Coupled Phase-Shift Model

For ES STAR RIS assisted communication systems with the coupled phase-shift model, the STAR beamforming design becomes quite challenging. This is because, for each STAR element, the transmission and reflection phase shifts are coupled. To facilitate the corresponding STAR beamforming design, an efficient element-wise based STAR beamforming approach is developed for minimizing the BS power consumption in a STAR RIS assisted single-input single-output two-user communication system [i.4]. As shown in Figure 5.3-2, the salient feature is that the phase-shift and amplitude coefficients of each STAR element are optimized one by one, i.e. in an element-wise manner. Therefore, the computational complexity only linearly scales with the number of STAR elements, which renders it promising to be used in practice since the size of STAR RIS is usually large.

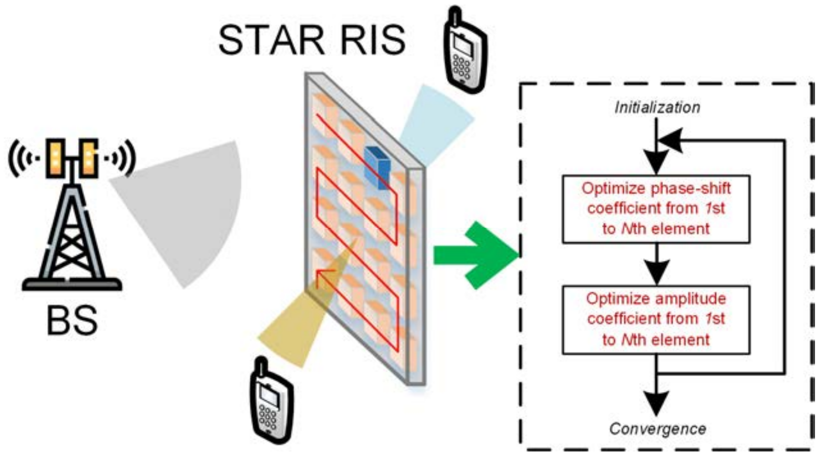

Figure 5.3-2: Element-wise based STAR beamforming design

5.3.3 Tile-based STAR Beamforming Design

The complexity of the passive beamforming design is a critical challenge for STAR RIS. Since the reconfigurable elements are not likely to have a power amplification function and the incident signal has experienced fading before arriving at the STAR RIS, the transmitted or reflected signal from each single element has limited energy. Hence, in order to ensure sufficient strength of the reflected signal, a large STAR RIS panel having a massive number of elements is necessary. Once an enormous number of elements are employed in the STAR RIS, the optimization complexity of their transmission and reflection coefficients will increase significantly, which leads to challenges on complexity of the beamforming.

A tile-based low-complexity beamforming approach can be employed to empower the STAR RIS, where the elements on STAR RIS are partitioned into several tiles [i.6]. The elements in the same tile, also as known as subsurface, have the same transmission and reflection coefficients. The tile-based beamforming approach no longer requires the STAR RIS controller to calculate reconfigurable coefficients for each element. The STAR RIS controller only needs to plan reconfigurable coefficients for each tile, thereby reducing the complexity of signalling, control circuitry, and computing required by STAR RIS beamforming.

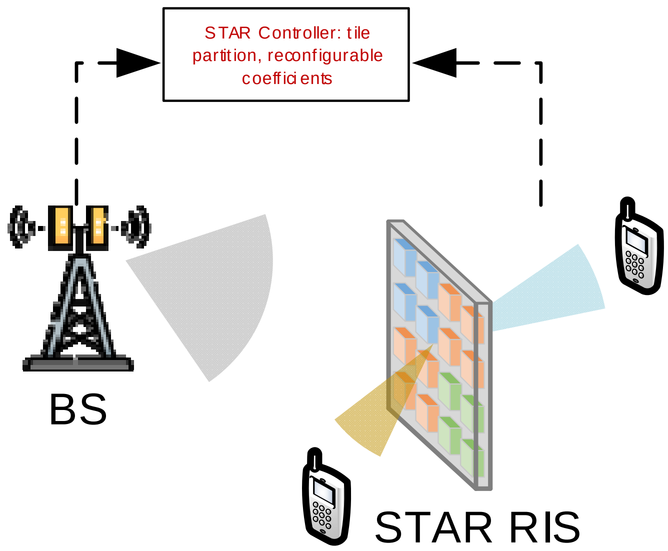

Figure 5.3-3: Tile based STAR RIS beamforming design

Specifically, the tile-based beamforming for two STAR RIS operating protocols, ES and SS are shown as below. As shown in Figure 5.3-4(a), for ES protocol, each tile has transmission and reflection capabilities. The size, shape, and element partitioning of the tile can be flexible or fixed depending on the specific case. In contrast, in the SS protocol, each tile can selectively work in transmission or reflective modes.

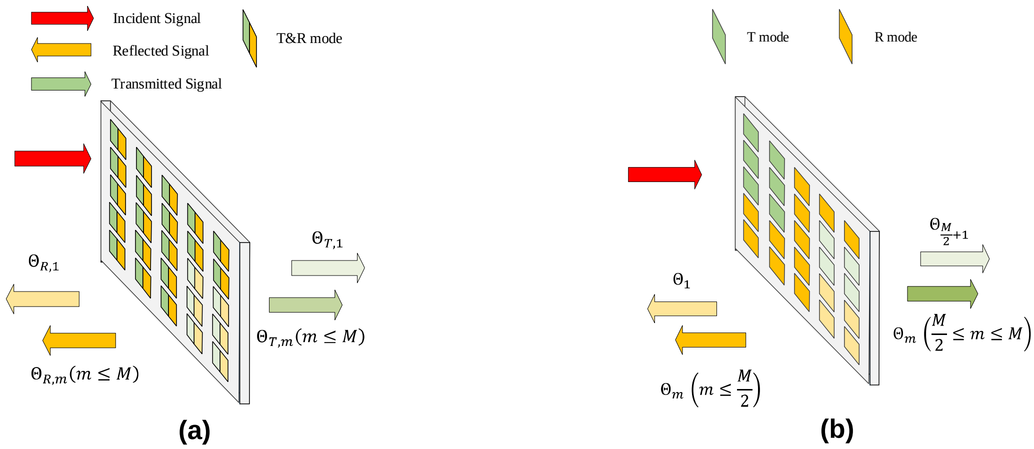

Figure 5.3-4: Tile based STAR RIS beamforming design (a) ES protocol. (b) SS protocol

5.4 Deployment Considerations

Considering STAR RIS as more advanced type of RIS, they can be primarily considered for deployment scenarios where typical reflecting-only or transmit (refract)-only RIS cannot fully serve the intended coverage region. Compared to reflecting-only or transmit (refract)-only RIS, the key benefit of STAR RIS is that they can be leveraged to provide close to 360-degree coverage, i.e. both the front region and back region of the RIS surface can be served with STAR RIS.

One of the important deployment scenarios for STAR RIS could be to extend both outdoor coverage and outdoor-to-indoor coverage using the same RIS, as illustrated in Figure 5.4-1. In the deployment scenario illustrated in Figure 5.4-1, the RIS could either be deployed on a window or it could be integrated on the wall of the building. In the case where the RIS is deployed on a window, depending on the implementation, it may allow light to pass through, or not.

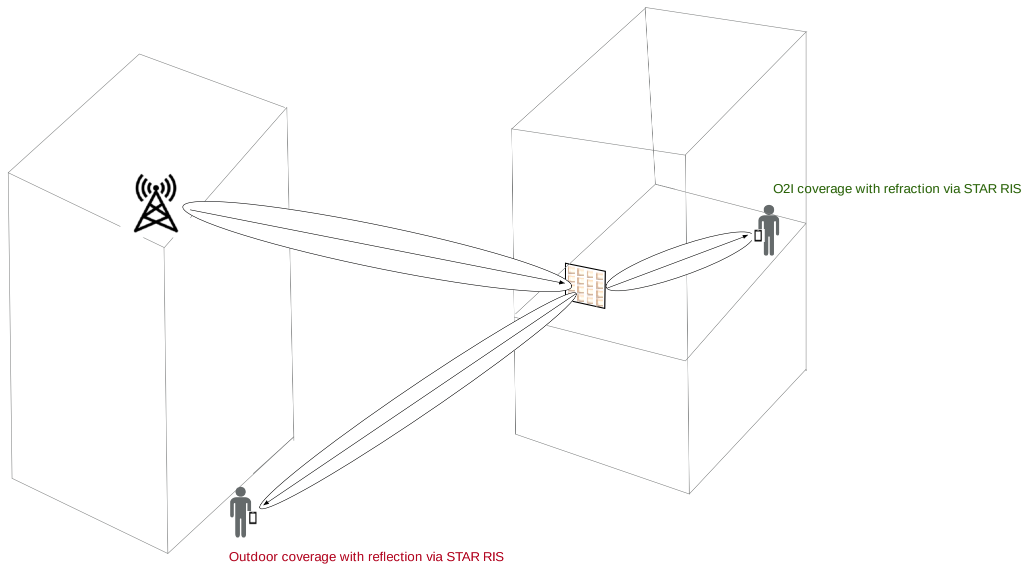

Figure 5.4-1: Illustration of STAR RIS deployment for outdoor and O2I coverage with same RIS

Furthermore, STAR RIS could possibly operate in different modes, e.g. energy-split mode, where transmit (refract) and reflect happen simultaneously; or time-split mode, where transmit (refract) and reflect happen at different time instances. One mode maybe more suited than the other mode depending on the use-cases. Energy-split mode with simultaneous transmission and reflection would be beneficial for channels/signals that need to be transmitted to multiple users, such as broadcast, multicast, and group-common channels/signals. For example, it could be beneficial to have STAR RIS operating either in ES mode for transmission of synchronization signal blocks, i.e. the same SSB beam transmitted from the base station is transmitted (refracted) and reflected at the same time via STAR RIS or beam sweeping of SSB via STAR RIS in TDM manner.

One of the most promising applications of STAR RIS is to enlarge the coverage area and improve the quality of wireless transmissions, especially when the links between the BSs or access points and users are severely blocked (e.g. by trees along roads, buildings, and metallic shells of vehicles). As shown in Figure 5.4-2, the deployment of STAR RIS can be divided into three scenarios, namely outdoor, outdoor-to-indoor, and indoor, as these are identified as three important scenarios for RIS deployment and testing [i.5]:

- **Outdoor:** In outdoor scenarios, similar to conventional reflecting-only RISs, STAR-RISs can be mounted on building facades and roadside billboards to create additional communication links. More innovatively, STAR RIS can also be accommodated by the windows of vehicles (e.g. cars, aircraft, and cruise ships) to enhance the signal strength received inside by exploiting their transmission capability, thus extending the coverage area/quality of BSs and satellites.

- **Outdoor-to-Indoor:** It is usually challenging to serve indoor users with outdoor BSs since the severe penetration loss caused by building walls gravely restricts the coverage provided by outdoor BSs, especially in mmWave bands. In fact, STAR RIS constitutes an efficient technique for creating an outdoor-to-indoor bridge as illustrated in the middle of Figure 5.4-2. STAR RIS can serve users both indoors and outdoors by simultaneously reflecting and transmitting signals to both directions.

- **Indoor:** For indoor communications, STAR RIS is more appealing than conventional reflecting-only RISs. As conventional reflecting-only RISs merely achieve half-space coverage, the signals emerging from the AP may require multi-hop bounces for reaching the target user. However, by exploiting both transmission and reflection, the resultant full-space coverage may reduce the propagation distance, thus increasing the received signal power.

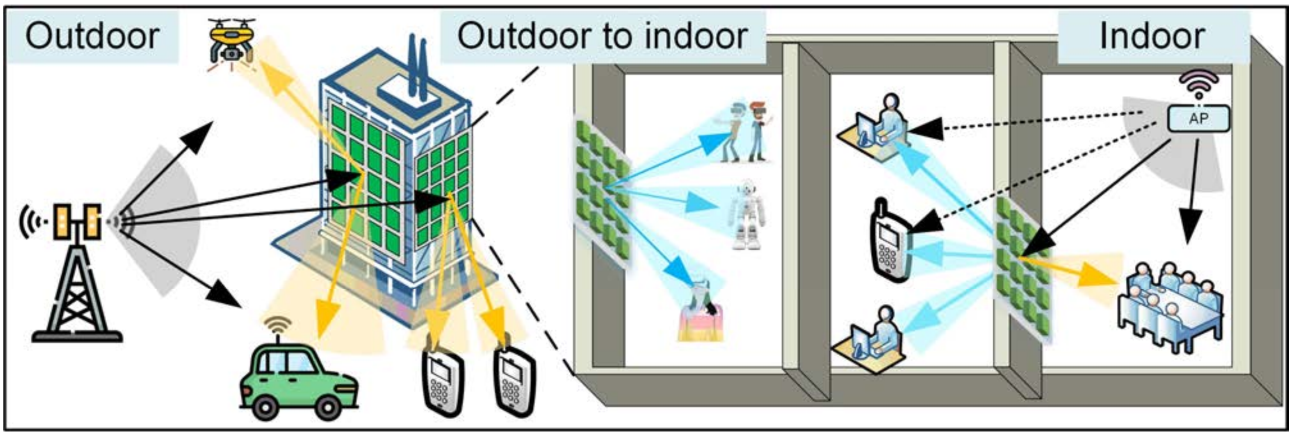

Figure 5.4-2: Illustration of deploying STAR RIS for wireless coverage extension

5.5 Resource Allocation Schemes

5.5.1 STAR RIS aided transmission-reflection NOMA

As recommended by IMT-2030, NOMA and RIS are important technique for mobile services in the years 2030 and beyond. For NOMA to achieve a high performance gain over orthogonal multiple access, it is important to pair users having different channel conditions. However, for conventional reflecting-only RISs, the benefits of NOMA may not be fully reaped since the channel conditions of users in the local reflected space are generally similar. Exploiting STAR RIS facilitates a more beneficial communication framework, namely transmission-reflection NOMA, where a pair of users at the transmission- and reflection-oriented side can be grouped together for supporting NOMA, as shown in Figure 5.5-1. For example, the reflected and transmitted signals can pertain to a high-date rate video streaming user and a low-date rate Internet-of-Things user, respectively. By optimizing the transmission and reflection coefficients of STAR RIS, sufficiently different transmitted and reflected channel conditions can be achieved, thus enhancing the NOMA gain. As a result, the STAR RIS aided transmission-reflection NOMA resource allocation framework is well suited to support the heterogenous quality-of-service requirements of the two types of users.

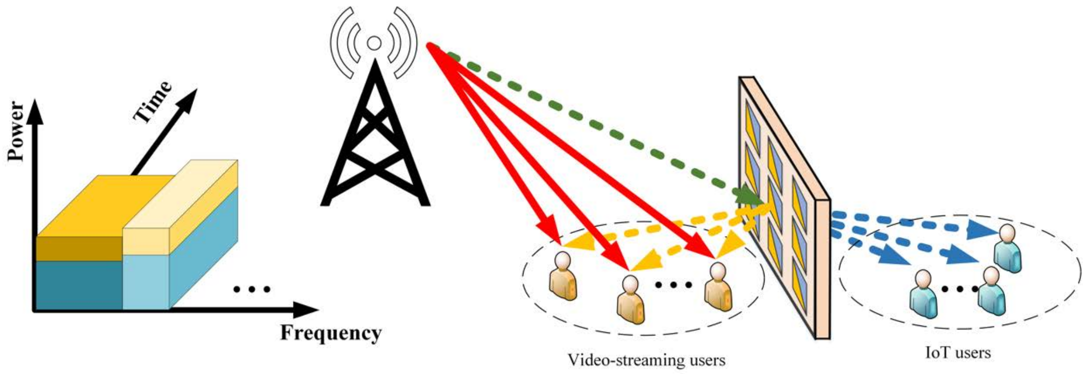

Figure 5.5-1: STAR RIS aided transmission-reflection NOMA

5.5.2 STAR RIS aided NCJT

For realistic multi-cell communication networks, the performance of cell-edge users cannot be guaranteed due to the strong inter-cell interference. NCJT can be exploited to enhance the quality of experience of cell-edge users. In Figure 5.5-2, a beneficial STAR RIS-aided NCJT resource allocation scenario is presented. In particular, several multiple-antenna BSs are coordinated to serve a cell-edge user. Additionally, each BS can also individually serve an additional cell-centre user. A STAR RIS is deployed in each cell where the cell-edge user is located in the transmission half space, while the cell-centre user is located in the reflection half-space. The advantages of this resource allocation scheme are that on one hand, the received SINR of the cell-edge user can be enhanced through NCJT and the design of the transmission coefficients of all STAR RISs, while on the other hand, the reflection coefficients of each STAR RIS can be optimized for enhancing the performance of the cell-edge user.

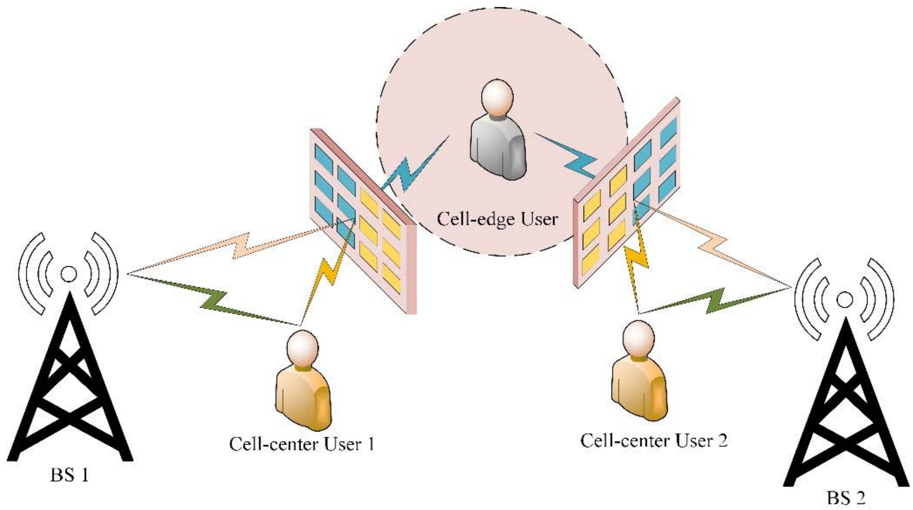

Figure 5.5-2: STAR RIS aided NCJT

5.6 Performance Analysis

5.6.1 Diversity Analysis

Consider a frequency-flat narrowband communication system with a single-antenna Tx, two single-antenna Rxs, and a STAR RIS consisting of M elements. One Rx is located at the transmission region of STAR RIS, and the other Rx is located at the reflection region of STAR RIS. Perfect CSI is assumed, and the independent phase-shift model is considered for STAR RIS. Let $h_i \in \mathbf{C}^{1\times 1}$ denote the channel coefficient of Tx-to-Rx channel, $\boldsymbol{g} \in \mathbf{C}^{M\times 1}$ denote the channel vector from Tx to STAR RIS, $\boldsymbol{r}_i \in \mathbf{C}^{M\times 1}$ denote the channel vector from STAR RIS to Rx, and $\boldsymbol{\Theta}_i = \mathrm{diag}\left(\sqrt{\beta_1^i}e^{j\theta_1^i},\ldots,\sqrt{\beta_m^i}e^{j\theta_m^i},\ldots,\sqrt{\beta_M^i}e^{j\theta_M^i}\right)$ denote the reconfigurable coefficient matrix of STAR RIS. Here, $i \in \{t,r\}$ indicates the transmitted or reflected Rx. The end-to-end channel gain of Rx i is given by:

$$|z_i|^2 = |h_i + \boldsymbol{r}_i^H \boldsymbol{\Theta}_i \, \boldsymbol{g}|^2.$$

Under the target SNR for Rx i ($\bar{\gamma}_i$), the outage probability can be expressed as:

$$P_{out,i}(\bar{\gamma}_i) = \Pr\left\{|z_i|^2 < \frac{\bar{\gamma}_i \sigma_0^2}{p_i}\right\},$$

where p_i is the signal power allocated for Rx i and σ_0^2 is the received noise power. The diversity order of Rx i defined through the outage probability is given by:

$$D_i = -\lim_{p_i\to\infty} \frac{\log P_{out,i}(\bar{\gamma}_i)}{\log p_i}.$$

For STAR RIS, the maximum achievable diversity orders of the two Rxs are $D_t = D_r = M + 1$. Therefore, the total diversity order on the two sides of STAR RIS is $D_t + D_r = 2M + 2$.

To compare the performance between STAR RIS and conventional transmitting/reflecting-only RIS, the baseline is considered as follows. A composite RIS consists of one transmitting-only RIS with M_t elements and one reflecting-only RISs with M_r elements. Here, $M_t + M_r = M$. For this baseline, the maximum achievable diversity orders of Rx t and Rx r are $\bar{D}_t = M_t + 1$ and $\bar{D}_r = M_r + 1$, respectively. Therefore, the total diversity order on the two sides of the composite RIS is $\bar{D}_t + \bar{D}_r = M + 2$.

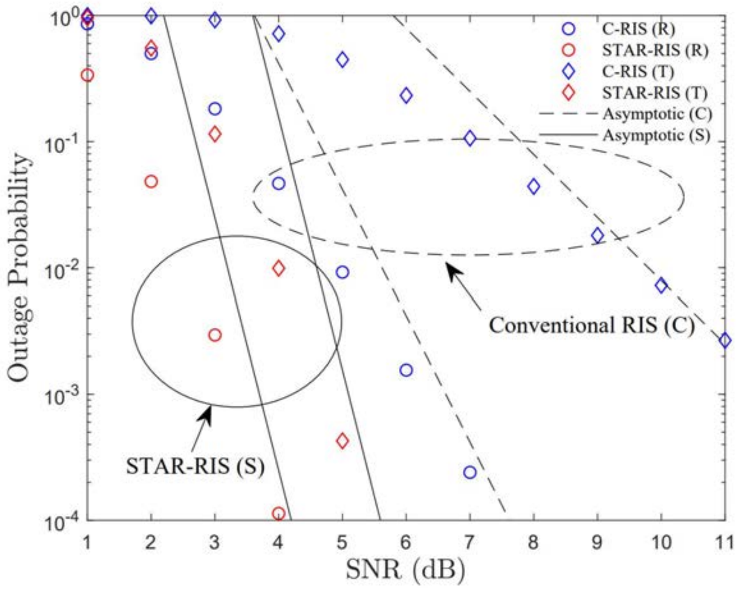

Figure 5.6-1: Outage probabilities of STAR RIS and conventional transmitting/reflecting-only RISs

Figure 5.6-1 illustrates the outage probabilities and diversity orders of STAR RIS and conventional transmitting/reflecting-only RISs. The red markers represent the simulated outage probability for the two Rxs assisted by a STAR RIS with $M = 8$ elements. The amplitude coefficients for transmission and reflection are 0,4 and 0,6. The blue markers represent a conventional transmitting/reflecting-only RISs with $M_t = 3$ and $M_r = 5$ elements. The numerical results shows that the simulated outage probabilities fit well with the analytical asymptotic results. The diversity orders of Rxs of STAR RIS and conventional transmitting/reflecting-only RISs are consistent with the analytical results. Both Rxs can achieve full diversity orders for STAR RIS, while cannot for conventional transmitting/reflecting-only RISs.

5.6.2 STAR Beamforming Optimization for Power Minimization

Consider a frequency-flat narrowband communication system with a 2-antenna Tx, two single-antenna Rxs, and a STAR RIS consisting of M elements. One Rx is located at the reflection region of STAR RIS, and the other Rx is located at the reflection region of STAR RIS. As shown in Figure 5.6-2(a), the direct Tx-to-Rx links are assumed to be blocked, and only the STAR RIS transmission/reflection-side Tx-to-Rx links are available. Perfect CSI is assumed for beamforming design. Rician fading channels are used for Tx-STAR RIS and STAR RIS-Rx channels and the Rician factor is 3 dB. The path loss exponent is 2.2, the path loss at a reference distance of 1 meter is -30 dB, and the noise power is -90 dBm. The Tx sends different messages to different Rxs. The active beamforming at the Tx and the STAR beamforming employing the three operating protocols are jointly optimized for minimizing the transmit power required to satisfy the target Rx rates. Let $\boldsymbol{g} \in \mathbf{C}^{M\times 1}$ denote the channel vector from Tx to STAR RIS, $\boldsymbol{r}_i \in \mathbf{C}^{M\times 1}$ denote the channel vector from STAR RIS to Rx, and $\boldsymbol{\Theta}_i = \mathrm{diag}\left(\sqrt{\beta_1^i}e^{j\theta_1^i}, \ldots, \sqrt{\beta_m^i}e^{j\theta_m^i}, \ldots, \sqrt{\beta_M^i}e^{j\theta_M^i}\right)$ denote the reconfigurable coefficient matrix of STAR RIS. For STAR RIS in ES and SS protocols, the achievable communication rate of Rx $i \in \{t, r\}$ is given by:

$$R_i^{ES/SS} = \log\left(1 + \frac{\left|\boldsymbol{r}_i^H \boldsymbol{\Theta}_i^{ES/MS}\, \boldsymbol{g}\boldsymbol{w}_i\right|^2}{\left|\boldsymbol{r}_i^H \boldsymbol{\Theta}_i^{ES/MS}\, \boldsymbol{g}\boldsymbol{w}_{\bar{i}}\right|^2 + \sigma_0^2}\right),$$

where $\bar{\iota} = r$, if $i = t$; and $\bar{\iota} = t$, otherwise. $\boldsymbol{w}_i$ denotes the active beamforming vector for Rx i. For STAR RIS in TS, the achievable communication rate of Rx $i \in \{t, r\}$ is given by:

$$R_i^{TS} = \lambda_i \log\left(1 + \frac{\left|\boldsymbol{r}_i^H \boldsymbol{\Theta}_i^{TS}\, \boldsymbol{g}\boldsymbol{w}_i\right|^2}{\lambda_i \sigma_0^2}\right),$$

where λ_i denotes the time fraction allocated for Rx $i \in \{t, r\}$.

For comparison, the full-space coverage is achieved by employing one conventional reflecting-only RIS and one transmitting-only RIS, each of which has $M/2$ elements. Figure 5.6-2(b) shows that, independent of the adopted operating protocols, STAR RIS always outperforms conventional transmitting/reflecting-only RISs. Regarding the performance of STAR RIS with different operating protocols, TS achieves the best performance for the two-Rx setup. This is because TS achieves interference-free communication for each Rx by exploiting the time domain.

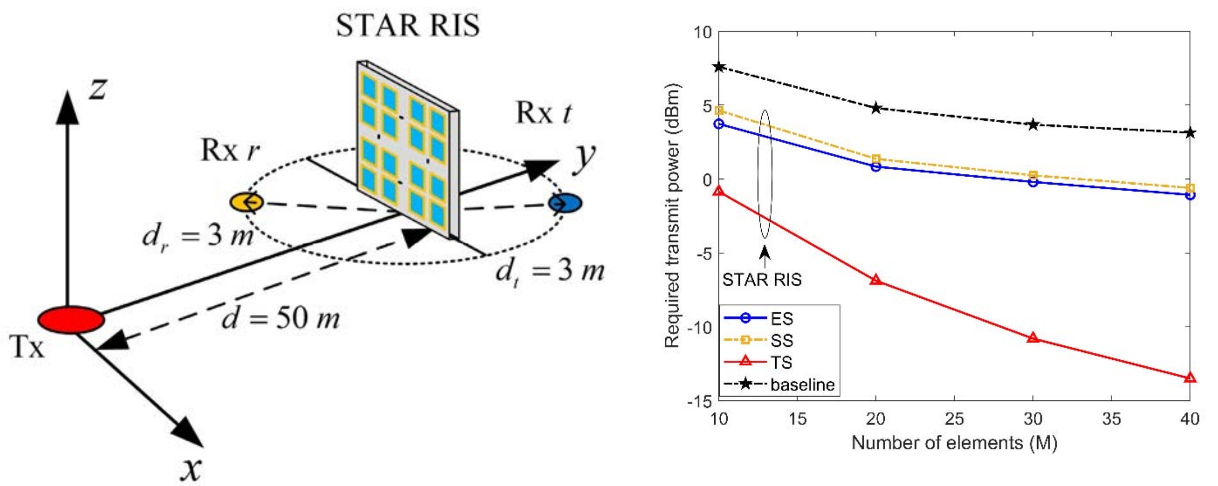

(a) The simulated setup **(b) Power consumption versus M**

Figure 5.6-2

6 RIS with sensing capabilities

6.0 General Introduction

The RIS with sensing capabilities can create virtual LoS links between the BS and the sensing targets, which is beneficial for scenarios where the direct links between them are blocked. Moreover, the RIS utilizes a large aperture to counter the effects of signal attenuation and boost the received echo signal strength for more accurate detection. As shown in Figure 6.0-1, different RIS architectures have been employed in the wireless sensing systems, namely, the passive RIS, semi-passive RIS, and active RIS [i.7]. The passive RIS only comprises a number of passive reflective elements that reflect signals to the target and echoes to the BS. Its sensing performance is largely limited because the system suffers severe signal attenuation after multiple reflections, i.e. the BS-RIS-target-RIS-BS link. The semi-passive RIS consists of a number of additional active sensors, which directly receive and process the target echo signals, thereby enabling the signals to travel through fewer hops. The active RIS is equipped with passive reflecting elements, dedicated active sensors, and a transmitter controlled by the controller. In this case, the transmitter enables the transmission of probing signals, which makes it similar to a traditional radar station. Although this is beneficial for sensing, it incurs not only greater hardware expenses and energy usage at the RIS but also complicated and effective interference cancellation techniques, which may severely constrain the application scenarios of active RIS-enabled sensing in practice.

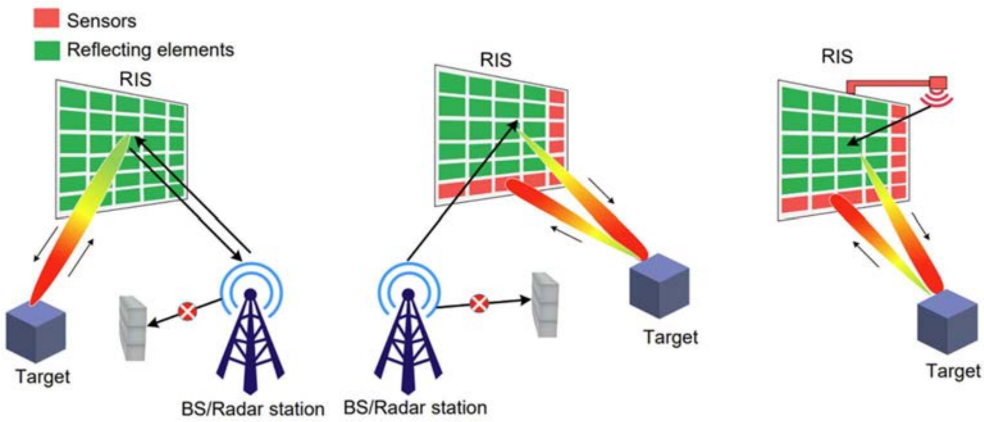

(a) Passive RIS **(b) Semi-passive RIS** **(c) Active RIS**

Figure 6.0-1: Illustration of three architectures of RIS-assisted sensing systems

6.1 Signal and Channel Model

The communication begins with a pilot signal to estimate the $k'th$ UE location through the calculation of AoAs. Assuming that the metasurface contains sensors either directly integrated alongside the reflecting cells or placed independently, the sensing matrix **H** can be formed, which corresponds to the measured phase difference between the *i'th* and *(i + 1)'th* sensor for the *j'th* incident angle. In other words, **H** is an $M \times N$ real-valued matrix with $M + 1$ sensed samples and N AoAs. The phase difference vector g is weighted by H:

$$w = \mathbf{H}^T g.$$

The column of $\mathbf{H}^T H$ that has the smallest distance from w corresponds to the estimated AoA. For a j'th column of $\mathbf{H}^T H$, denoted as h_j , the column with the minimum distance J_{est} is calculated as:

$$J_{est} = arg \min_{j=1 \ldots N} ||w - h_j||_2,$$

where $||.||_2$ is the Euclidean norm. Once J_{est} is known, the unknown AoA can be estimated based on reference AoAs in the sensing matrix.

Given the estimated UE location, the RIS can optimize its channel gain to each UE_k with SINR given as:

$$SINR_k = \frac{\left|\left(h_k^H \boldsymbol{\Theta G} + h_{D,k}^h\right) w_k\right|^2}{\sigma_n^2 + \sum_{j \neq k} \left|\left(h_k^H \boldsymbol{\Theta G} + h_{D,k}^H\right) w_j\right|},$$

where w_k is the transmit precoder of UE_k, $h_{D,k}^H$is a LoS link between BS and UE (if exists), h_k^H is the reflected link through the RIS, G is the LoS link between BS and RIS, and $\boldsymbol{\Theta}$ is the RIS matrix with $(\theta_1, \dots, \theta_N)$ reflection coefficients.

Given the $SINR_k$, the MF-RIS will optimize its configuration with the goal of maximizing the sum rate for each UE:

$$R = \sum_{k=1}^{K} log_2(1 + SINR_k).$$

The strategy is to maximize the intensity of $h_k^H \boldsymbol{\Theta G}\, w_k$, which corresponds to enhancing the channel gain and is approximately equal to maximizing $SINR_k$. Once the optimization is complete, the RIS becomes independent of the BS precoding and relies only on the array response vectors towards the BS and UE.

6.2 Operating Protocols

6.2.0 General

Operating protocol is the prerequisite of the RIS design including the sensing algorithms, beamforming, deployment, and resource allocation. In the following, two basic sensing protocols for general RISs: sensing-at-BS and sensing-at-RIS, will be introduced, followed by a further discussion about the operating protocol design for STAR RIS to facilitate the integration of the communication and sensing functions.

6.2.1 Sensing at the BS and RIS

For any type of RIS, there are two generic operating protocols based on where the sensing signal is captured and processed: sensing-at-BS and sensing-at-RIS [i.8]. Typically, these protocols utilize different RIS hardware architectures illustrated in Figure 6.0-1. Specifically, sensing-at-BS requires only a passive RIS deployed within the area of interest, while sensing-at-RIS necessitates dedicated sensors installed on the RIS to actively absorb the sensing signals. The key characteristics are elaborated as follows:

- **Sensing-at-BS:** This operating protocol can be regarded as a monostatic sensing protocol, where the transmitter and receiver are collocated. In this setup, the RIS can be seamlessly integrated as an add-on solution, establishing a virtual LoS path for targets in blind regions and serving as an additional reference point for sensing targets. This direct integration minimizes additional hardware costs for existing systems. However, this protocol also presents several challenges. The first challenge is the weak echo signal received at the receiver due to multiple reflections caused by the RIS. Additionally, the echo signals from different targets are merged in the RIS-BS link, which may complicate the algorithm design for multi-target sensing.

- **Sensing-at-RIS:** This operating protocol can be regarded as the bistatic sensing protocol, i.e. the transmitter and receiver are located at different places. This protocol addresses the key challenges encountered in the sensing-at-BS protocol. In this protocol, active sensors mounted on the RIS receive echo signals directly from the targets, ensuring that the signals are not merged. In this case, the design of the sensing algorithm can be significantly simplified. Additionally, by reducing the number of signal reflections from the transmitter to the receiver, the strength of the echo signals is considerably enhanced, enhancing the sensing accuracy.

6.2.2 STAR RIS Protocols for Integrated Sensing and Communications

An important consideration for the operating protocol design of RIS is to integrate Sensing and Communication (S&C) functions to meet the diverse requirements of next-generation wireless networks. To this end, STAR RIS appears to be a promising variant of RIS to facilitate the fusion of these two functions. A general discussion on exploiting RIS in ISAC systems can be found in clause 6.2.2 of ETSI GR RIS 002 [i.9]. This clause primarily focuses on how STAR RIS can facilitate ISAC through protocol design. In comparison to conventional reflection-only RISs, STAR RISs exhibit two distinctive attributes that can be harnessed for the design of ISAC systems. On the one hand, STAR RIS enables full-space coverage. Therefore, it can facilitate seamless communication and extensive sensing across the entire space, which is referred to as the *integrated full-space protocol* and depicted in Figure 6.2-1(a). On the other hand, STAR RIS also partitions the entire space into two separate spaces, namely the transmission and reflection space. This partition enables STARS to potentially accommodate communication and sensing functionalities within two separate half-spaces, which is referred to as the *separated half-space protocol* and depicted in Figure 6.2-1(b). The key characteristics of these two protocols are summarized in the following:

- **Integrated Full-Space Protocol:** The advantage of this protocol is straightforward, i.e. enabling ubiquitous coverage and enhancing the DoF for both S&C functions through simultaneous transmission and reflection beamforming. However, both transmission and reflection beamforming need to be designed for both S&C. In particular, S&C typically required different distinct beam configurations. For instance, the utilization of an isotropic beam proves advantageous for target detection, while directional beams are favorable for facilitating unicast communication. The optimization objectives also diverge between S&C, such as minimizing the Cramér-Rao bound for enhancing sensing accuracy and maximizing spectral efficiency for elevating communication effectiveness. Consequently, the joint S&C beamforming generally requires sophisticated beamforming optimization.

- **Separated Half-Space Protocol:** In this protocol, the transmission and reflection signals are responsible for communication and sensing, respectively. Therefore, individualized designs for communication and sensing beamforming at the STAR RIS become feasible, leading to a notable reduction in beamforming complexity. It is worth noting that achieving full-space S&C coverage is possible through the separated half-space protocol by utilizing two STAR RISs with different S&C half-space configurations.

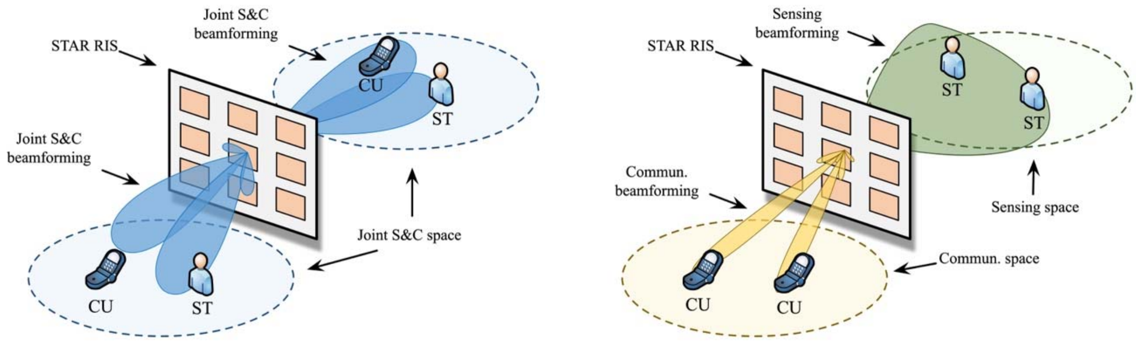

(a) Integrated full-space protocol **(b) Separated half-space protocol**

Figure 6.2-1: Illustration of operating protocols for STAR RIS in ISAC systems, where "CU" and "ST" stand for communication user and sensing target, respectively

6.3 Reconfigurable Coefficient Design

6.3.0 General

Reconfigurable coefficient design is significant for improving the sensing capability of RIS. RIS-aided sensing considers the performance metrics directly related to parameter estimation and/or target detection. Designing reconfigurable coefficients for the sensing capability requires different performance metrics than communication. Typically, there are two widely used design methods in sensing beamforming: beampattern-based design and theoretical-boundary-based design. These methods are generic for multi-functional RIS and there is no restriction on the type of RIS. Thus, in the following, the fundamentals of these two design methods are introduced using a conventional reflective RIS as an example.

6.3.1 Beampattern-based Design

The beampattern-based design aims to realize a sensing-preferred beampattern, i.e. how much power should be radiated in different directions. Focusing on a far-field scenario, the radiation power of RIS in a specific direction (φ, ϕ), where θ and ϕ are azimuth and elevation angles, respectively, can be expressed as follows:

$$P(\varphi, \phi) = \boldsymbol{a}^H(\varphi, \phi)\boldsymbol{R}_{\mathrm{RIS}}\boldsymbol{a}(\varphi, \phi),$$

where $\boldsymbol{a}(\varphi, \phi)$ denotes the array response vector for RIS in direction (φ, ϕ) and $\boldsymbol{R}_{\mathrm{RIS}}$ denotes the covariance matrix of the reflected signal at RIS. The covariance matrix $\boldsymbol{R}_{\mathrm{RIS}}$ in RIS systems is given by:

$$\boldsymbol{R}_{\mathrm{RIS}} = \boldsymbol{\Phi}\boldsymbol{G}\boldsymbol{R}\boldsymbol{G}^H\boldsymbol{\Phi}^H,$$

where $\boldsymbol{R}$ denotes the covariance of the transmit signal at the BS, $\boldsymbol{\Phi}$ is the diagonal RIS coefficient matrix, and $\boldsymbol{G}$ is the channel matrix between the RIS and BS. The robust beampattern-based design is to approximate a pre-designed beampattern, which is given by:

$$\underset{\boldsymbol{R},\boldsymbol{\Phi},\delta\geq 0}{\text{minimize}} \sum\nolimits_{(\varphi,\phi)\in S} |\ \delta D(\varphi, \phi) - \boldsymbol{a}^H(\varphi, \phi)\boldsymbol{R}_{\mathrm{RIS}}\boldsymbol{a}(\varphi, \phi)\ |^2$$

$$\text{s.t.} \quad \mathrm{tr}(\boldsymbol{R}) \leq P_0,$$

$$\boldsymbol{R} \succcurlyeq 0,$$

$$\left|\boldsymbol{\Phi}_{n,n}\right| = 1, \forall n = 1, \dots, N,$$

where $D(\varphi, \phi)$ is a pre-designed beampattern, $\delta \geq 0$ is a scaling factor, and P_0 is the transmit power budget of the BS. The above beampattern-approximation design exhibits a good compromise between resolution and robustness by adjusting the widths of beams.

6.3.2 Theoretical-boundary-based Design

6.3.2.0 General

The theoretical-boundary-based design aims to directly minimize or maximize the theoretical boundaries for target sensing. Compared to the beam pattern-based design, the theoretical-boundary-based method directly optimize the sensing performance, thus leading to a better sensing performance in general but at a cost of higher computational complexity [i.10]. For example, for parameter estimation, the CRLB is the optimization target usually adopted, which delineates the fundamental lower bound on the covariance matrix of any unbiased estimator of the parameters. As shown in Figure 6.3-1 as examples, the DoA and the time-domain response can be estimated under both the point and extended target cases, respectively.

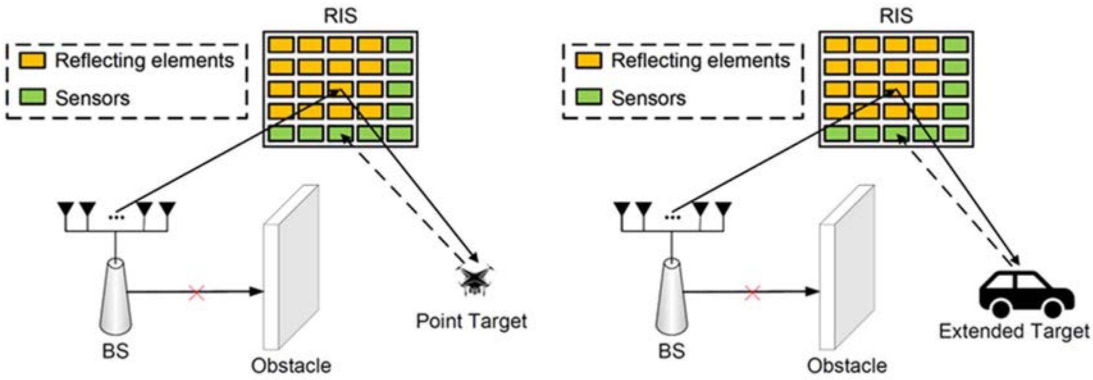

Figure 6.3-1: Illustration of two target models for sensing systems

6.3.2.1 Optimization Based RIS Beamforming Design

For RIS active sensing, RIS beamforming can be optimized over time by maximizing the average received signal power. Without any prior information, the resulting optimal RIS reflection design over time was shown to be an omnidirectional beampattern in the angular domain for scanning unknown targets in all possible directions. On the other hand, if given prior information on the region of the target location, RIS reflection can be more delicately devised to form a flat and wide beampattern uniformly covering the specific region of interest, thus increasing the received SNR for target localization. For RIS passive/semi-passive sensing, the RIS reflection, in general, needs to be jointly designed with the BS transmit beamforming to optimize the sensing performance, which renders the beamforming design problem more difficult to solve. For CRLB minimization for DoA estimation, a general RIS beamforming design problem can be expressed as:

$$\underset{\{\boldsymbol{R},\boldsymbol{\Phi}\}}{\text{minimze}} \quad \text{CRLB}(\boldsymbol{R},\boldsymbol{\Phi})$$

$$\text{s.t.} \quad \text{tr}(\boldsymbol{R}) \leq P_0,$$

$$\boldsymbol{R} \succcurlyeq 0,$$

$$\left|\boldsymbol{\Phi}_{n,n}\right| = 1, \forall n = 1, \dots, N.$$

Here, $\boldsymbol{R}$ represents the transmit covariance, $\boldsymbol{\Phi}$ denotes the RIS beamformer, and P_0 is the transmit power budget of the BS. The alternating optimization technique can be employed to sub-optimally solve the joint BS and RIS beamforming design problem by iteratively optimizing one beamforming with the other being fixed [i.11]. To further reduce the computational complexity, one can design the BS transmit beamformer so that it points toward the RIS, while RIS reflections can be dynamically tuned to maximize the received signal power at RIS sensors [i.12].

6.3.2.2 Codebook Based RIS Beamforming Design

The codebook-based RIS reflection design can also be explored to reduce the design complexity. For DoA estimation, the number of scanning beams formed by RIS should be large enough to cover the sensing area of interest. However, given the sum-/average-power constraint, this method can only support a small transmit power per beam. Alternatively, the hierarchical codebook-based RIS reflection design can be applied to balance the above trade-off. Specifically, RIS wide beams can be generated in the first phase to scan the entire area to determine the sector where the target is located. Then, in the second phase, RIS can steer narrow beams within this sector to further resolve the fine-grained target DoA.

6.4 Deployment Considerations

6.4.1 Target-mounted RIS

The deployment of RIS can significantly influence the sensing performance and even the sensing protocol design. In the following, a target-mounted RIS deployment strategy and the corresponding advantages and challenges will be introduced.

In sensing systems, the signal reflection at the target is typically random and can change rapidly in high-mobility scenarios. Apart from exploiting RIS to establish virtual LoS paths and enlarge the coverage area for sensing, controllable reflection of signals can be realized by mounting RIS on the target, as illustrated in Figure 6.4-1. In particular, the echo signal from the target can be crafted through the reflection beamforming of RIS. Moreover, if the STAR RIS is exploited, the signal impinged on the target can also go through the STAR RIS and provide additional communication service to the devices inside the target (e.g. mobile users in a vehicle) [i.13].

For this deployment strategy, through reflection beamforming, the echo signal can be dynamically adjusted to achieve maximum power directed toward the sensing node. This ensures that a stable and strong echo signal is consistently received at the sensing node, while also reducing the likelihood of detrimental multipath effects. Moreover, the incorporation of target-mounted RIS also facilitates the integration of sensing and communication. Specifically, by boosting the echo signal's strength, the sensing node can effectively track the target and acquire CSI of the LoS path in a pilot-free manner. This enables efficient communication to reliably convey information to the mobile user located within the target using STAR RIS transmission beamforming. However, establishing a control link between the sensing node and the target-mounted RIS is challenging due to the non-fixed position of the target. Therefore, a new control protocol for the RIS may be needed to facilitate the beamforming design.

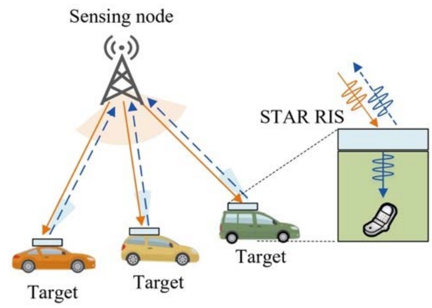

Figure 6.4-1: Target-mounted STAR RIS for ISAC

6.5 Resource Allocation Schemes

6.5.1 Joint Offline-Online Scheme

The resource allocation problem for RIS in sensing systems is more intricate than in communication systems due to two primary factors. First, while communication performance typically improves with higher SNR, sensing accuracy also depends on geometric considerations and the ability to differentiate signals from various paths. Second, estimating environmental parameters, such as ToA and DoA, necessitates distinct RIS reconfiguration strategies. For example, optimizing the RIS beam to maximize the SNR is sufficient for ToA estimation, while DoA estimation also requires considering the derivative of the SNR-maximizing beam [i.14]. Consequently, efficiently allocating time resources to these different reconfiguration strategies is essential for achieving optimal overall sensing performance. To address this complex resource allocation challenge, a joint offline-online scheme is introduced in the following.

In the offline phase, the resource allocation problem, e.g. transmit power and bandwidth allocation, at the BS is designed to account for the complex geometries of the deployment area. Since the instantaneous environment data is not available in this phase, the resource allocation design is under the assumption of random RIS reconfiguration and the objective of maximizing sensing coverage in terms of estimation error. The methods, such as exhaustive search and branch-and-bound, that can obtain the globally optimal solution but exhibit high complexity can be used in this phase, since there is no running time requirement in this stage. An example design result is shown in Figure 6.5-1.

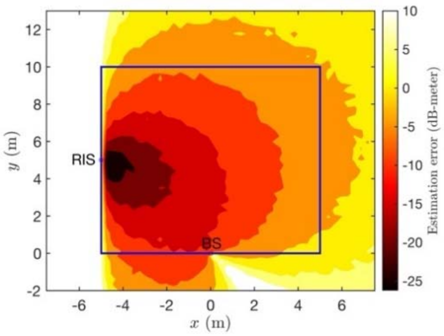

Figure 6.5-1: An example of offline-phase design that maximize the coverage in terms of estimation error

In the online phase, the time allocation and RIS reconfiguration selection problem are tackled to adapt to dynamic environments, building on the resource allocation design established for the BS during the offline phase. Additionally, there may be prior information available about the ROI in the online phase. As a result, only the sensing accuracy within this smaller ROI needs to be considered, significantly simplifying the problem compared to the offline phase and enabling more efficient real-time optimization.

6.6 Performance Analysis

6.6.1 Analysis Framework

There are two typical analysis frameworks for sensing systems, namely the Fisher information framework and the Shannon information framework. In the following, the pros and cons of these frameworks are discussed in sensing systems with RISs:

- **Fisher Information Framework:** Fisher information measures the amount of information an observation carries about specific unknown parameters, such as positions, velocities, and orientations. The inverse of Fisher information corresponds to the well-known CRLB discussed in clause 6.3.2, which represents the theoretical lower bound on the variance of an estimator. Thus, Fisher information is a valuable tool for analysing the estimation performance of unknown parameters in RIS sensing systems. Figure 6.6-1 illustrates an application of the Fisher information framework within the separated half-space protocol of STAR-RIS, introduced in clause 6.2.2, to assess the performance of target direction estimation. However, challenges may arise when both direct and RIS-reflected paths coexist between the BS and the target. In such cases, the high correlation of target parameters across both paths complicates the Fisher information, making it difficult to analyse.

- **Shannon Information Framework:** Shannon information is typically used in analysing the communication performance, but is proven to be also effective in reflecting sensing performance based on the rate-distortion theory [i.15]. Compared to the Fisher information, the Shannon information measures the general information, instead of information on specific unknown parameters, encapsulated within the sensing observation. Therefore, the Shannon information framework is valuable for analyzing the sensing performance of RIS systems in complex environments. However, the relationship between the Shannon information and the specific target parameters is not explicit.

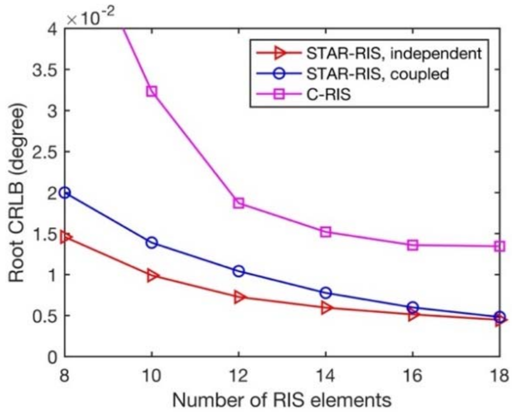

Figure 6.6-1: CRLB for estimating the target direction in the separated half-space protocol (see clause 6.2.2), achieved by STAR RIS with either independent or coupled phase shifts (see clause 5.1.1) and conventional RIS

7 RIS with Other Capabilities

7.0 General Introduction

The RIS can be further employed for enabling other capabilities within wireless networks. In the following, two types of MF-RIS, namely RIS with computing capabilities and RIS with caching capabilities are discussed.

7.1 RIS with Computing Capabilities

7.1.0 General

RIS with advanced hardware structures (e.g. multiple layers and STAR functions) can achieve powerful computing capability for wave-based signal processing.

7.1.1 Multi-Layer RIS Architecture with Computing Capabilities

The RIS can be further employed for enabling computing capabilities within wireless networks. RIS with advanced hardware structures (e.g. multiple layers) can achieve powerful computing capability for wave-based signal processing. The concept of SIM was recently proposed for realizing wave-based signal processing. As shown in Figure 7.1-1, the typical SIM consists of multiple layers of transmissive RIS and each layer has massive number of tunable elements [i.16]. SIM is generally used at transceivers to replace conventional large-scale analog arrays. By appropriately configuring these elements, the EM waves from the baseband can be manipulated through each layer, thus accomplishing advanced computation and signal processing tasks, such as MIMO precoding/combining, multi-user interference mitigation, and wireless sensing. Compared to conventional arrays at transceivers, the advantages of SIM are summarized as follows:

- **High-performance Computational Efficiency:** In contrast to conventional MIMO transceivers relying on digital signal processors, the SIM achieves precoding and combining as the EM wave propagates through multiple layers. Such a wave-based signal processing greatly reduces the computational time and complexity as well as enables parallel computational operations.

- **Low Hardware Cost and Energy Consumption:** In contrast to massive MIMO relying on a large number of active components, the wave-based signal processing of SIM can reduce the number of required RF chains and also does not rely on high-resolution digital-to-analog converters and analog-to-digital converters. Therefore, the energy consumption can be further reduced.

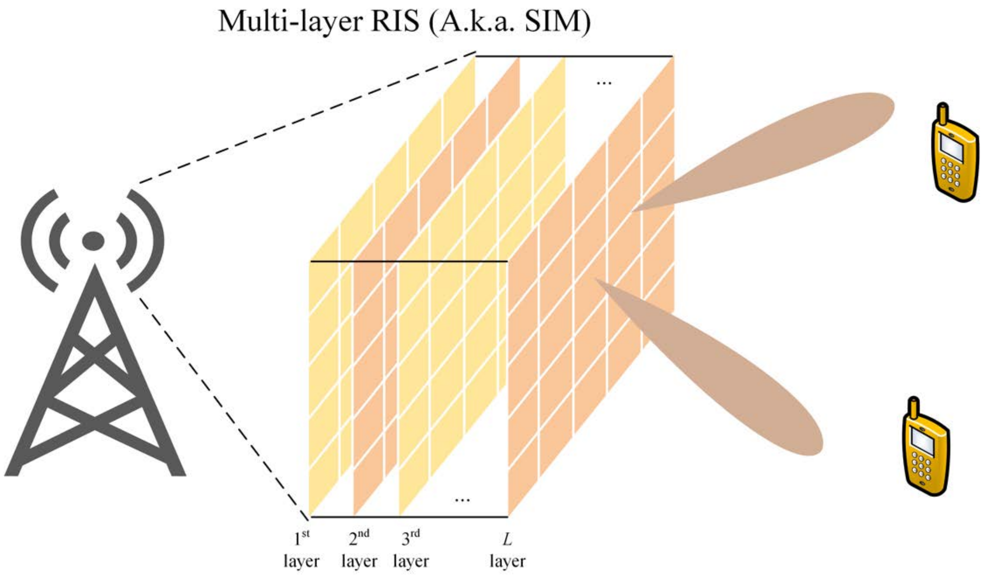

Figure 7.1-1: Multi-layer RIS (SIM) for wave-based signal processing (computing)

7.1.2 STAR RIS Architecture with Computing Capabilities

Conventional RISs face the challenge of reflecting both desired and interfering signals, resulting in unwanted reflections and degraded signal quality at the receiver. Overcoming this limitation necessitates a transition to RIS systems capable of performing both communication and computation. For example, the computing and beamforming functionalities can be enabled through a computational layer built with neuromorphic or Wave Domain Computing metamaterials in a STAR RIS Metasurface for integrated communication, computation, and sensing. The conceptual design of a STAR RIS is shown in Figure 7.1-2.

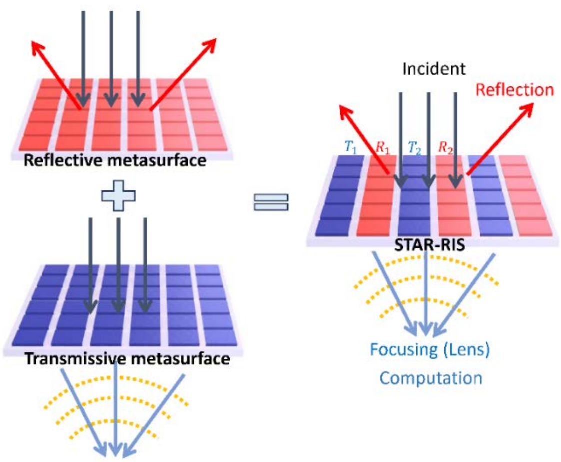

Figure 7.1-2: Operation of a STAR RIS with reflection and computational capability

When an incoming wave impinges on the STAR RIS, part of it is reflected for communication, while the transmitted portion, shaped by a lens phase profile, performs Fourier transformations in the $k-$domain enabling computational tasks. By using a coding metasurface, the STAR RIS achieves tailored beamforming for communication via reflection and Fourier transform operations for AoA estimation via transmission, by performing the Discrete Fourier Transform function:

$$X[k] = \sum_{n=0}^{N-1} x(n)e^{\frac{-j2\pi kn}{N}},$$

where N is the number of sampled points and k is the wave vector. This concept is illustrated in Figure 7.1-3.

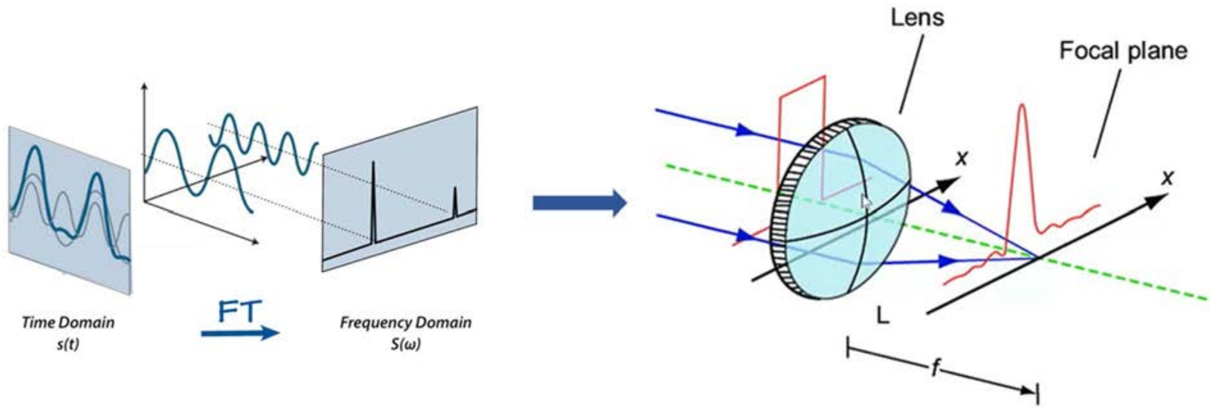

Figure 7.1-3: STAR RIS acting as a lens for DFT computing

Discrete Fourier Transform (DFT) establishes a connection between the time (space) domain and the frequency (wave vector) domain, which can be used for applications in radio signal processing and analysis. This function can be implemented as shown in Figure 7.1-4, on a STAR metasurface with a linear phase gradient in the reflection space and a lens phase profile in the transmission space, enabling dual functionality without requiring stacked arrays or specialized metamaterials. In this example, the metasurface is designed to operate at 26 GHz.

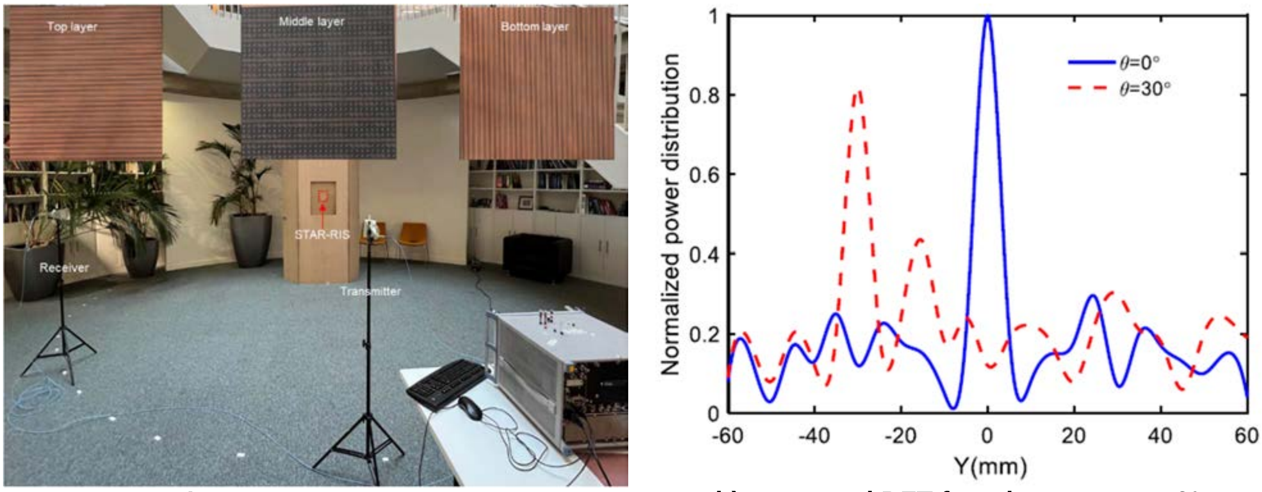

a) measurement setup

b) measured DFT function output at 0° transmission angle and the 30° reflection angle of the wireless signal

Figure 7.1-4: Fabricated STAR RIS

7.2 RIS with Caching Capabilities

Deploying caches at network edge nodes, such as BSs or roadside units is regarded as a promising technology to reduce content transmission redundancy and network traffic load. As RIS is typically deployed on the network edge nearing the user equipment, expanding the edge cache on it can effectively reduce the distance of data transmission. For RIS with caching capabilities, a single-antenna transmitter with cache storage can be installed at RIS to send content cached to users. Since the transmitter is near the RIS panel, it can utilize the reconfigurable array elements on the RIS to achieve beamforming, which ensures the efficiency of the cached content delivery.

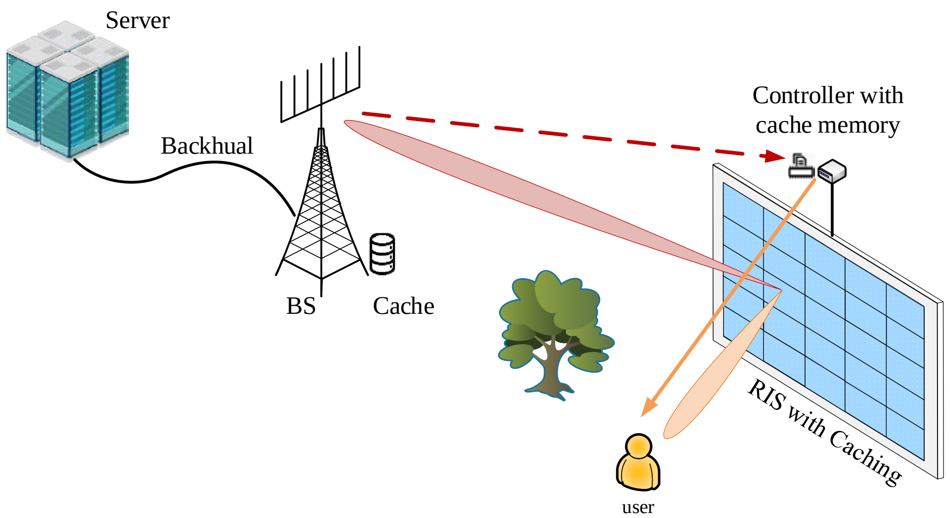

Figure 7.2-1: RIS with caching capabilities

As displayed in Figure 7.2-1, the RIS with caching capabilities deploys a memory and micro transmitter on the RIS. The storage is connected to the BS via a wired link, and it can cache some popular content, such as video, images, and speech. When a user requests content cached by RIS, the caching transmitter and RIS panel will work together to deliver the content to the user equipment over the wireless channel.

Designing a joint decision for caching management and beamforming on caching at RIS poses challenges. Firstly, the cache state of RIS and BS need to be jointly scheduled to avoid the cache waste, maximizing the cache hit rate. Furthermore, the beamforming of RIS needs to fully consider whether the cache transmitter is activated. When the BS and the cache deployed on RIS work simultaneously, RIS has to be able to provide appropriate passive beamforming for both signals. Since this problem is a long-term optimization problem and it requires RIS to identify the current working status, the deep reinforcement learning is an effective solution [i.17]. This artificial intelligence solution can identify the current channel status, cache status, and user request to give joint decisions for cache update and beamforming for RIS.

8 Conclusion

The present document summarizes the views of ETSI ISG RIS on the development of MF-RIS, including STAR-RIS, RIS with sensing capabilities, RIS with computing capabilities, and RIS with caching capabilities, as well as the corresponding coefficient designs, deployment considerations, and the performance analysis. The contents can serve as a reference point for relevant specifications and standards to study and model RIS-integrated systems.

History

Document history		
V1.1.1	June 2025	Publication